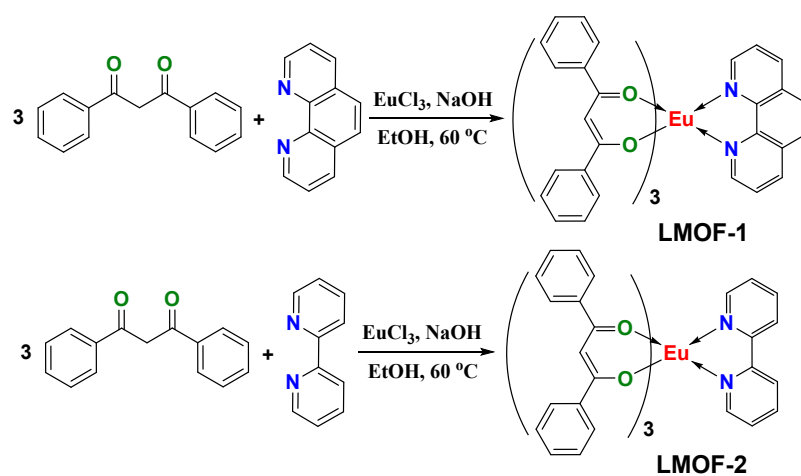


## Supporting Information

### A simple photoluminescent strategy for pH and amine vapors detection based on Eu(III)-complex functionalized material

#### Table of Contents

1. The synthesis route of LMOF-1 and LMOF-2 (**Scheme S1**)
2. MS,  $^{13}\text{C}$  NMR,  $^1\text{H}$  NMR and FTIR spectra (**Fig. S1-S8**)
3. The absorption, excitation and emission spectra (**Fig. S9-S12**)
4. Detection under different pH conditions in solution (**Fig. S13**)
5. Verification of the responsive mechanism (**Fig. S14** and **Scheme S2**)
6. Preparation of the functionalized films and test device (**Fig. S15** and **S17**)
7. Detection of pH and vapors with the prepared materials (**Fig. S18-S23**)
8. The SEM spectra of LMOFs (**Fig. S24-S25**)



**Scheme S1.** The synthetic route of LMOF-1 and LMOF-2.

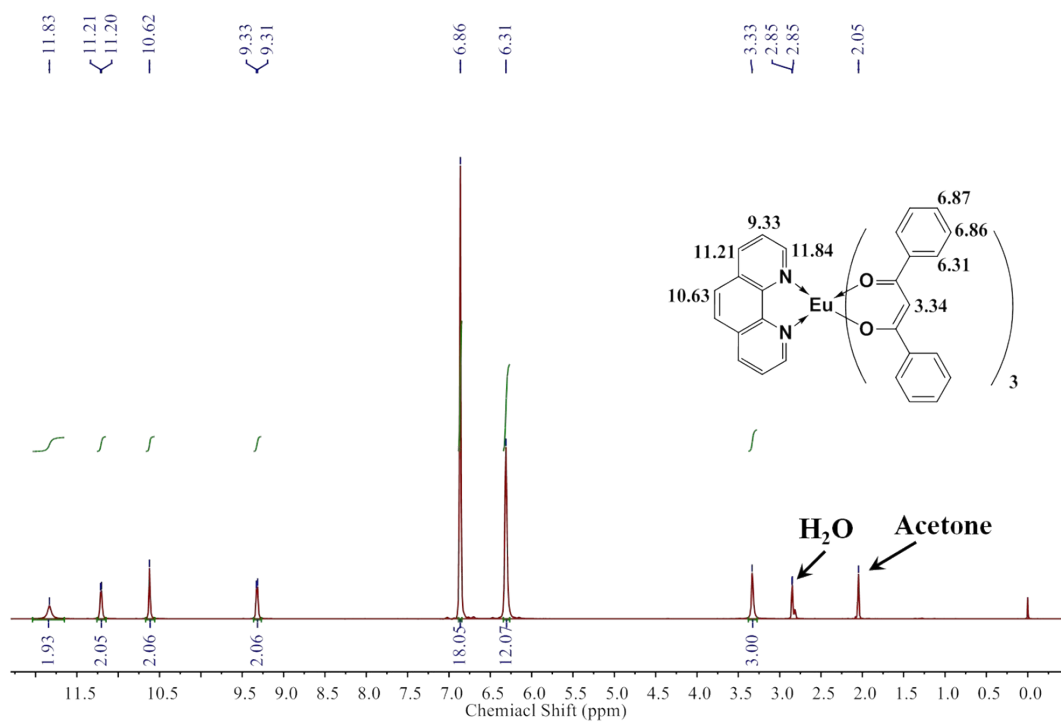


**Fig. S1.** The <sup>1</sup>H NMR spectrum of LMOF-1 (acetone-*d*<sub>6</sub>, 500 MHz).

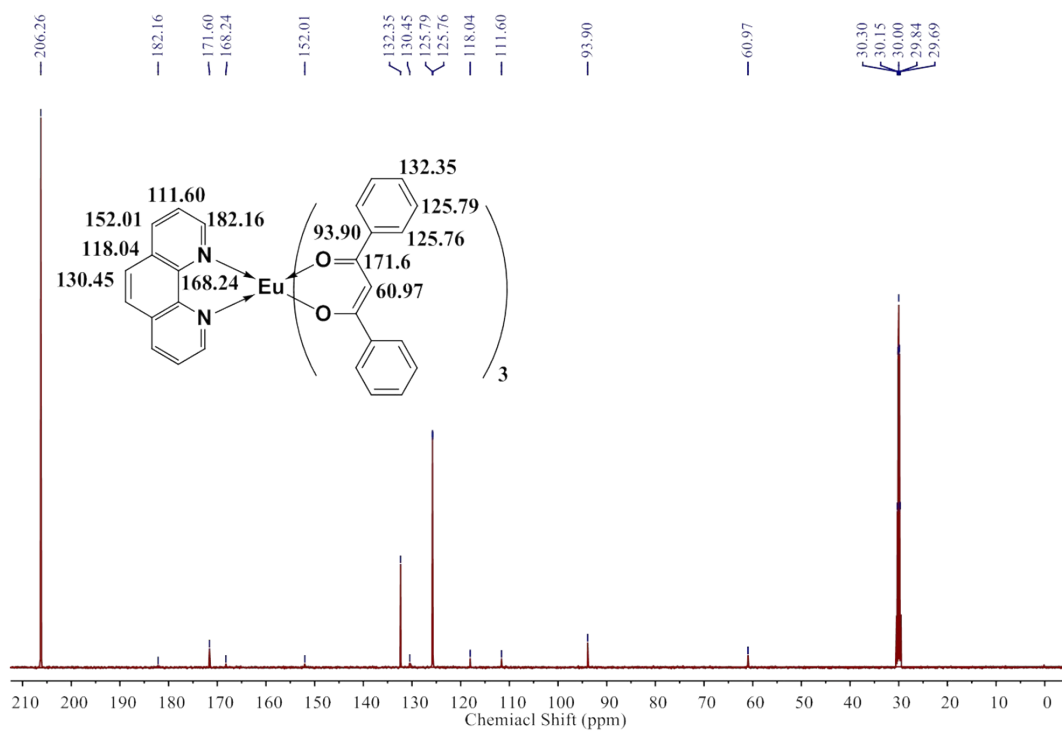


**Fig. S2.** The  $^{13}\text{C}$  NMR spectrum of LMOF-1 (acetone- $d_6$ , 125 MHz).

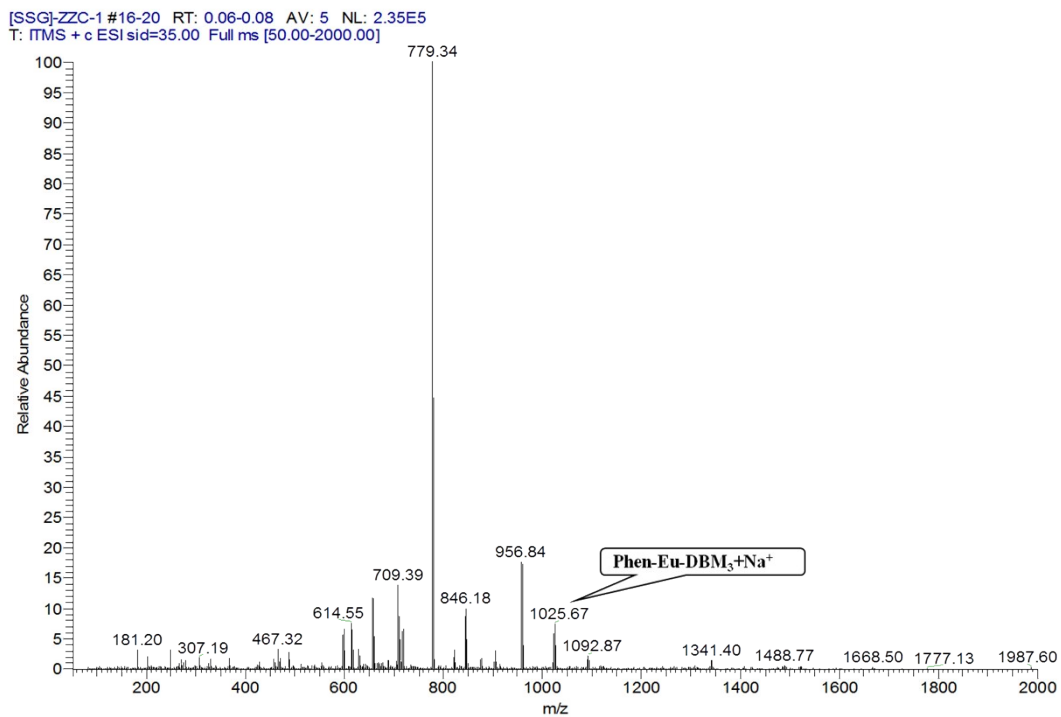


**Fig. S3.** ESI-MS spectrum of LMOF-1.

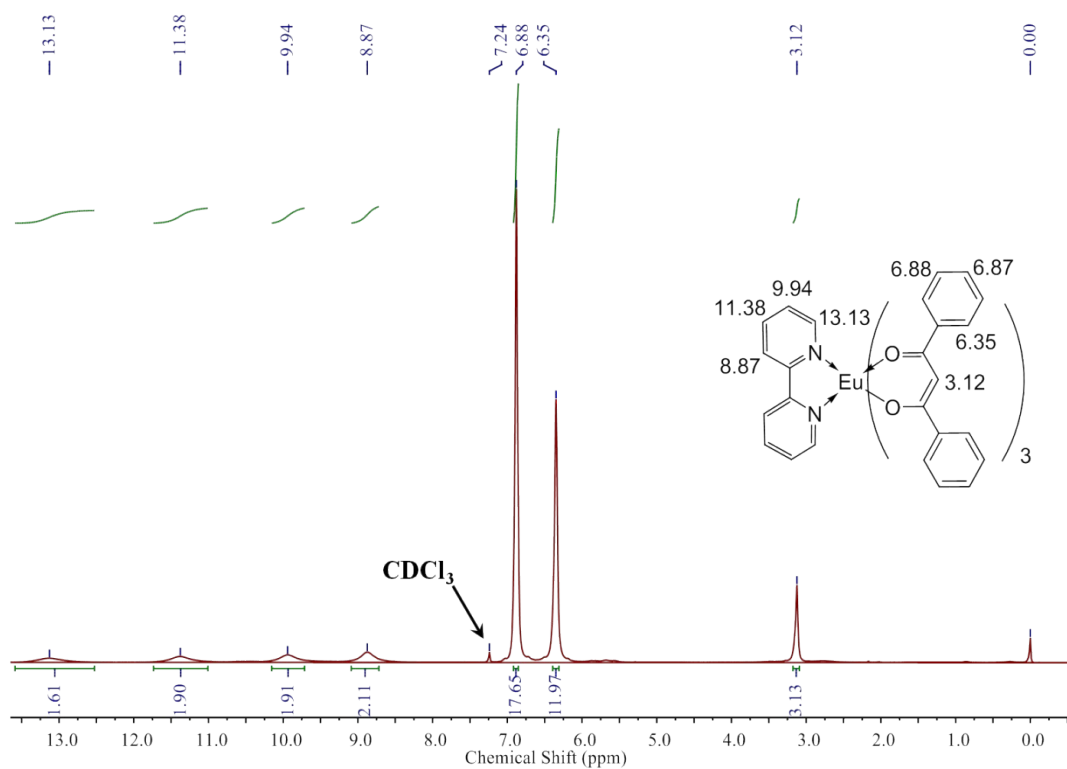


**Fig. S4.** The <sup>13</sup>C NMR spectrum of LMOF-2 (CDCl<sub>3</sub>, 500 MHz).

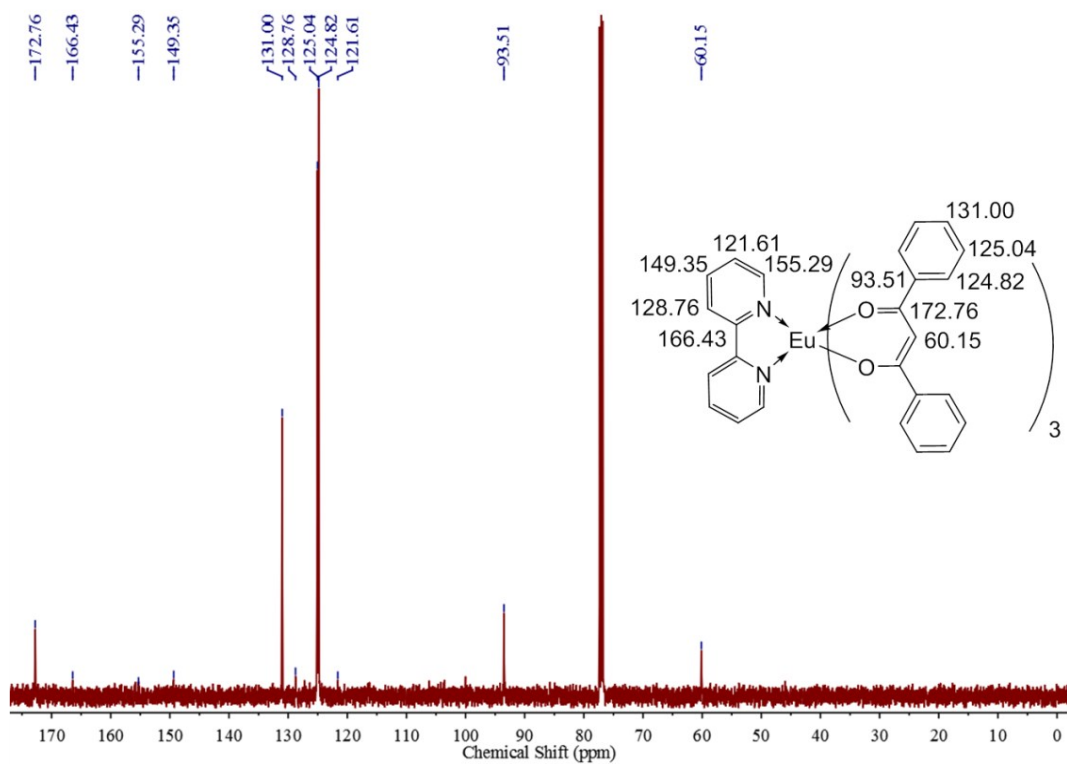


**Fig. S5.** The <sup>13</sup>C NMR spectrum of LMOF-2 (CDCl<sub>3</sub>, 125 MHz).

[SSG]-BPY-11 #167-195 RT: 1.30-1.42 AV: 29 NL: 3.37E4  
T: ITMS + c ESI Full ms [50.00-2000.00]

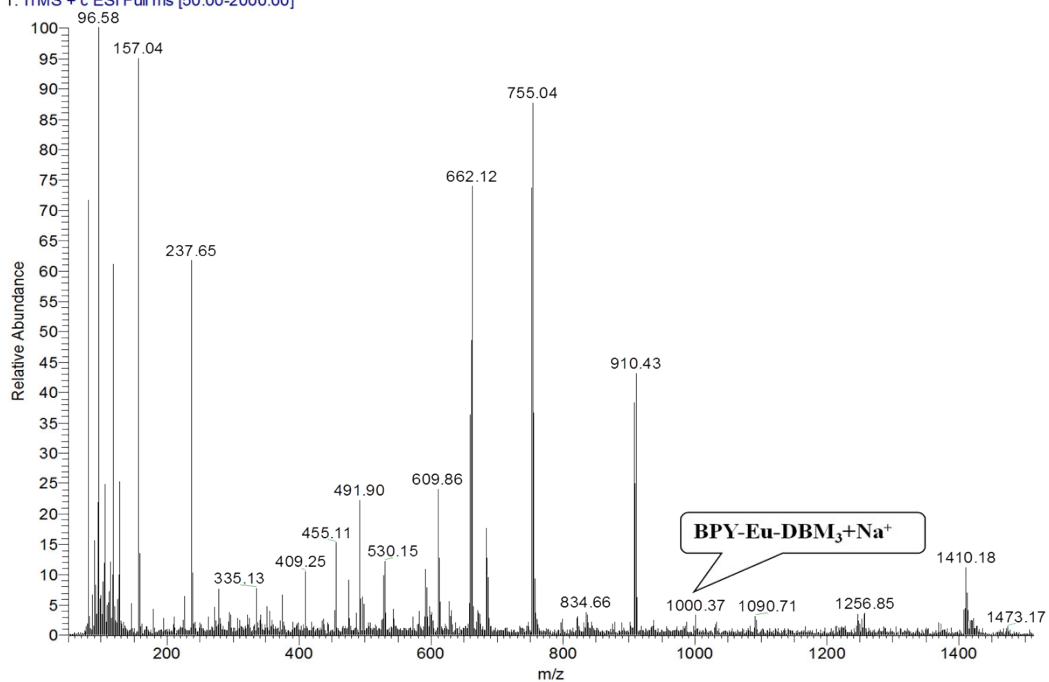


Fig. S6. ESI-MS spectrum of LMOF-2.

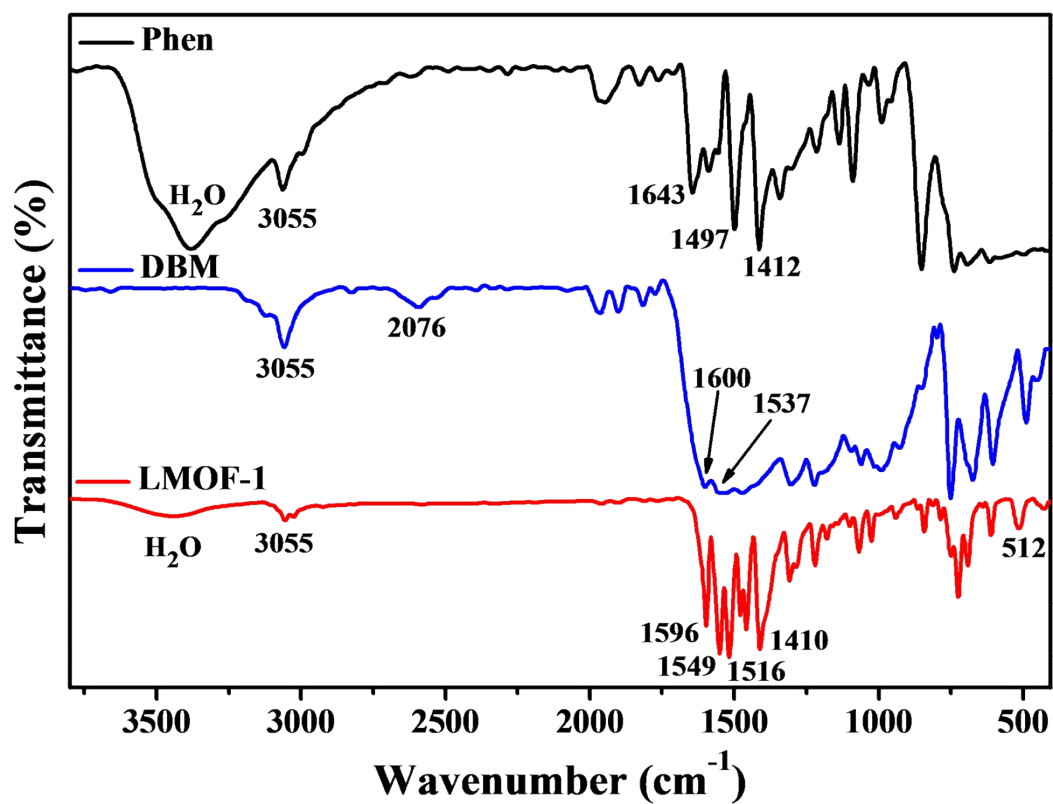


Fig. S7. The IR spectra of Phen, DBM and LMOF-1.

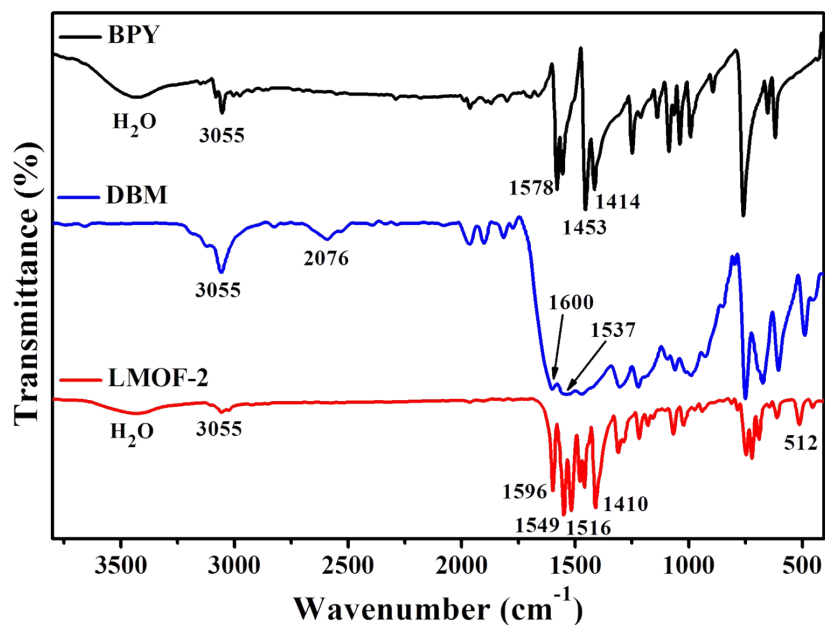


Fig. S8. The IR spectra of BPY, DBM and LMOF-2.

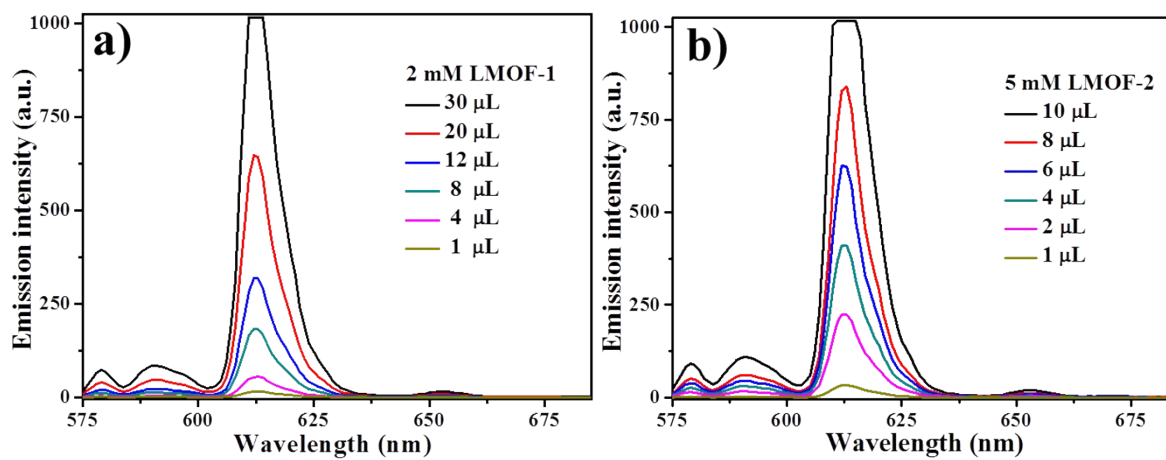
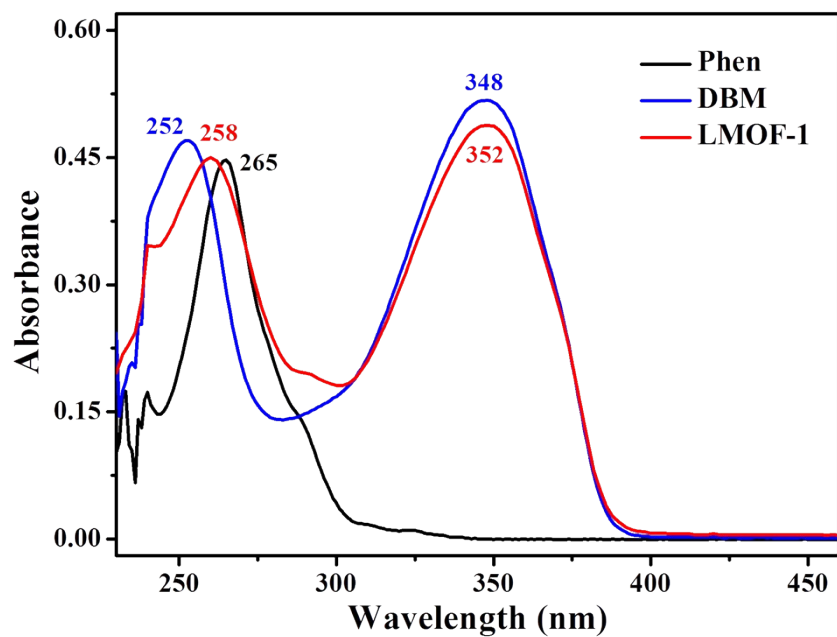
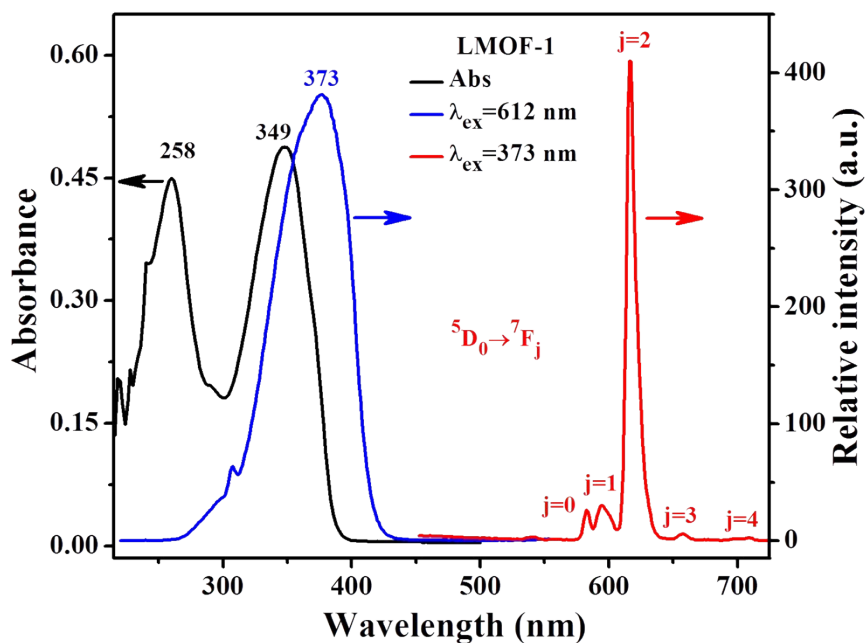


Fig. S9. a) The emission spectra of LMOF-1 with different added volume to solution ( $\text{H}_2\text{O}/\text{DMSO}$ ,  $v/v=5/1$ ,  $\text{pH}=11$ ,  $\lambda_{\text{ex}}=375$  nm). b) The emission spectra of LMOF-2 different added volume to solution ( $\text{H}_2\text{O}/\text{DMSO}$ ,  $v/v=5/1$ ,  $\text{pH}=11$ ,  $\lambda_{\text{ex}}=385$  nm).



**Fig. S10.** UV-vis absorption spectra of Phen (12  $\mu\text{M}$ ), DBM (30  $\mu\text{M}$ ) and LMOF-1 (8  $\mu\text{M}$ ) were recorded in mixed solution of H<sub>2</sub>O/DMSO (V/V=5/1).



**Fig. S11.** The absorption, excitation and emission spectra of LMOF-1 (8  $\mu\text{M}$ ) were recorded in mixed solution of H<sub>2</sub>O/DMSO (V/V=5/1).

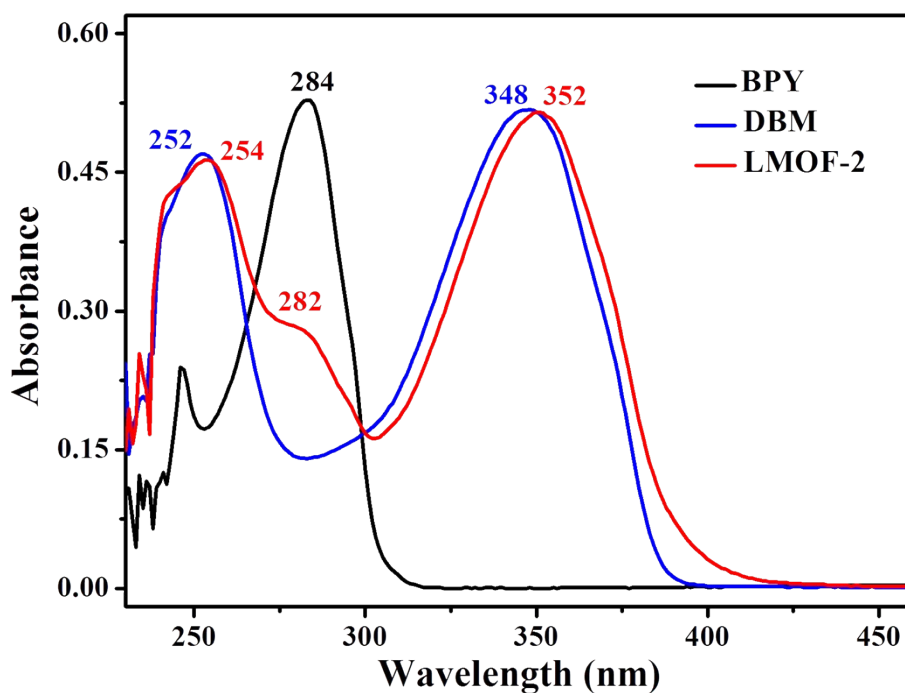


**Fig. S12.** The UV-vis absorption spectra of BPY (40  $\mu\text{M}$ ), DBM (30  $\mu\text{M}$ ), and the LMOF-2 (10  $\mu\text{M}$ ) were recorded in mixed solution of  $\text{H}_2\text{O}/\text{DMSO}$  (V/V=5/1).

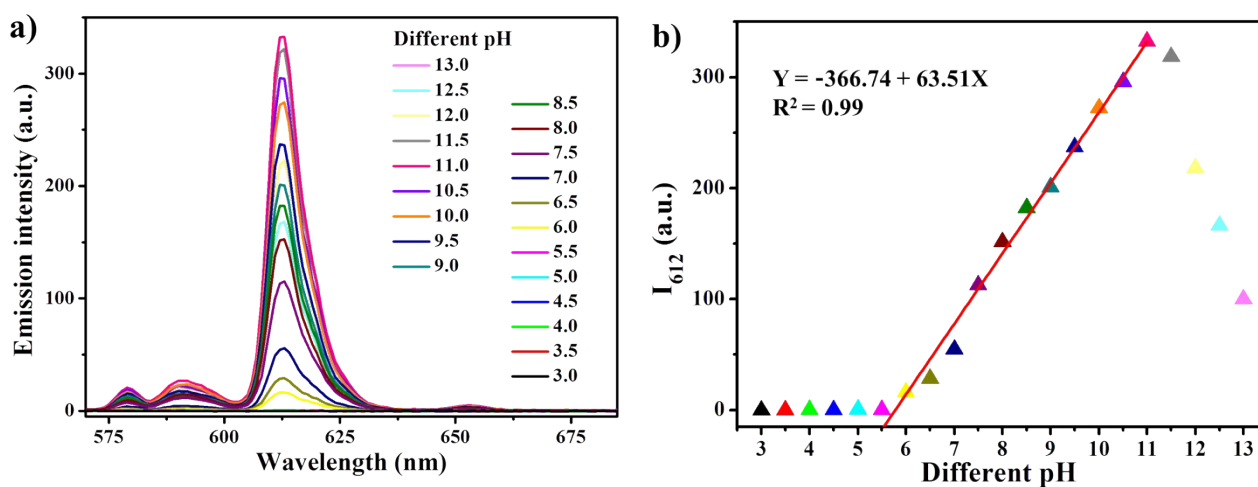


**Fig. S13.** a) The emission spectra of LMOF-1 (8  $\mu\text{M}$ ) under different pH conditions in solution ( $\text{H}_2\text{O}/\text{DMSO}$ , v/v=5/1). b) Relationship between the emitting intensity at 612 nm and pH values ( $\lambda_{\text{ex}}$ =375 nm, slits: 3/3 nm).



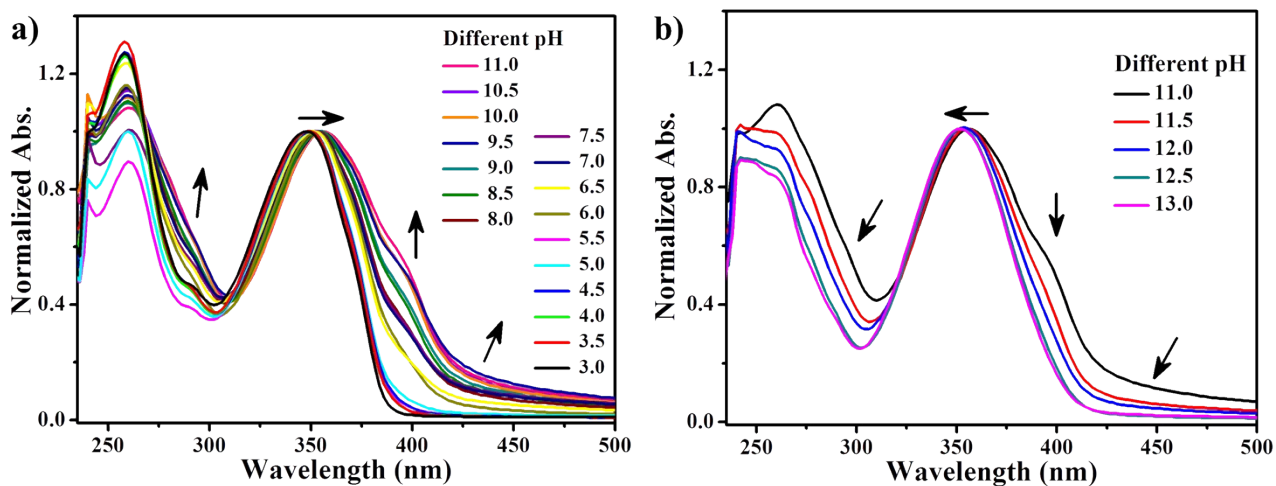
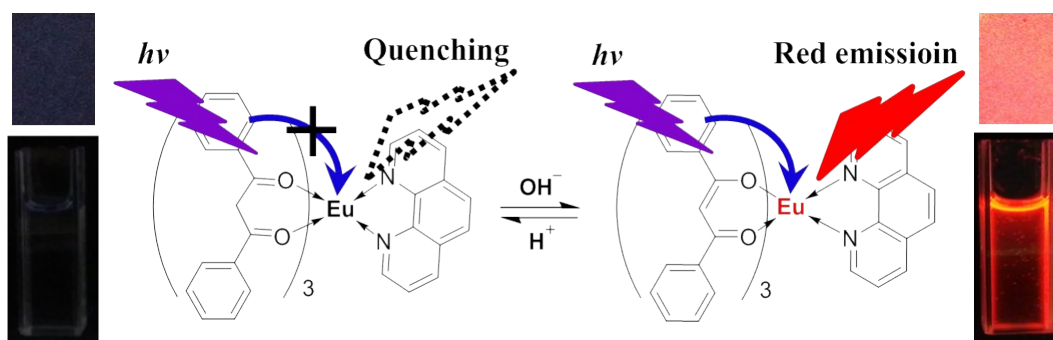


Fig. S14. Normalized absorption spectra of LMOF-1 (8  $\mu\text{M}$ ) under different pH conditions in solution ( $\text{H}_2\text{O}/\text{DMSO}$ ,  $v/v=5/1$ ).



Scheme S2. The response mechanism of the LMOF-1 to different pH.

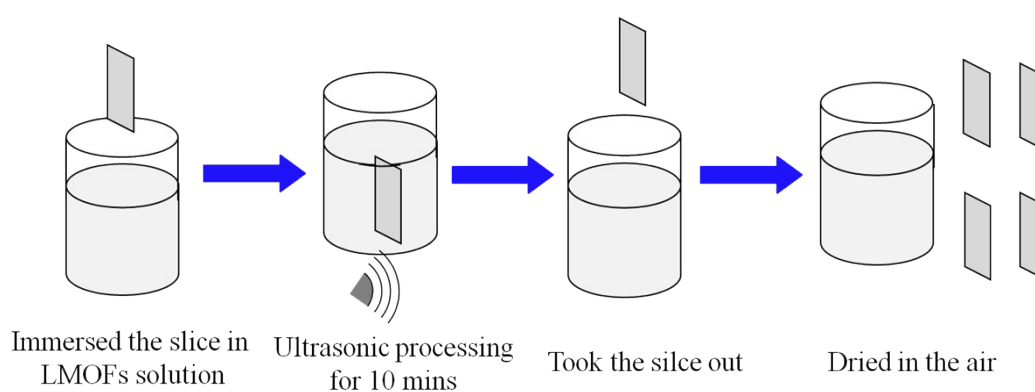
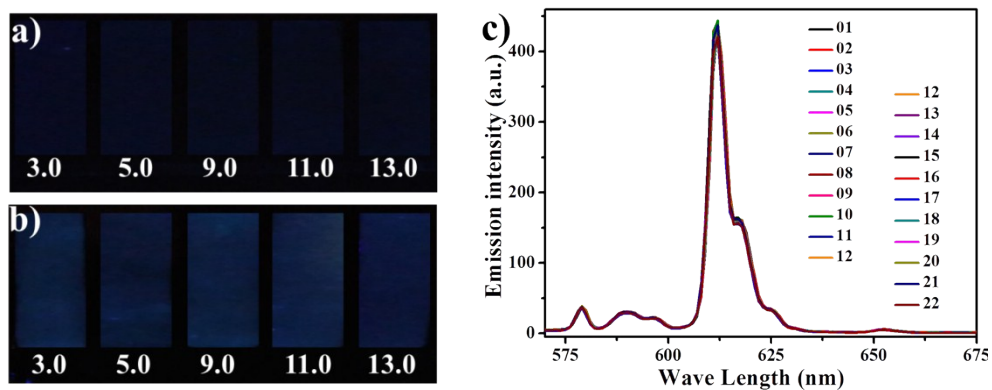
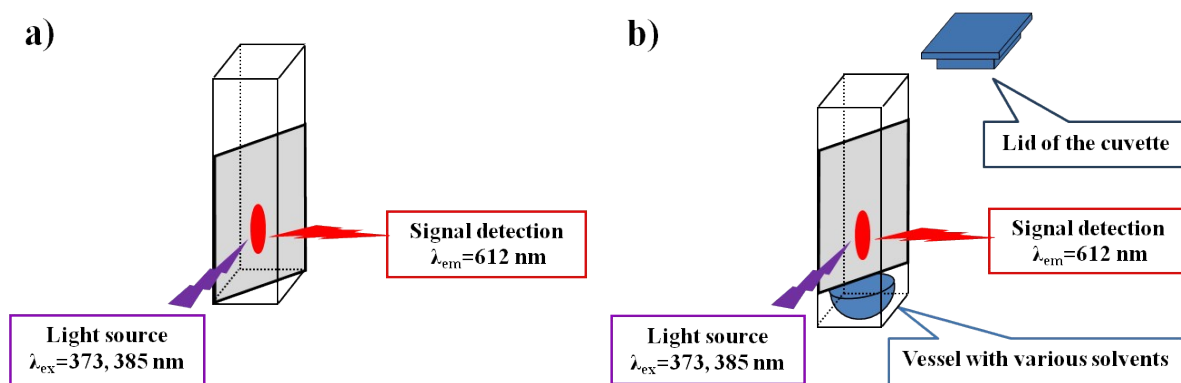


Fig. S15. The processes of LMOFs-based functionalized films prepared in the solution of LMOFs and PVA.



**Fig. S16.** The digital photos of silica plates **a)** and filter paper **b)** without LMOFs treated with different pH solutions under UV light (365 nm). **c)** The luminescence intensity of LMOFs-based functionalized films (22 groups contrastive experiment) were relatively uniform.



**Fig. S17.** The sensor setup used for measurement the photoluminescence of films after processing different pH solutions **a)** and vapors **b)**.

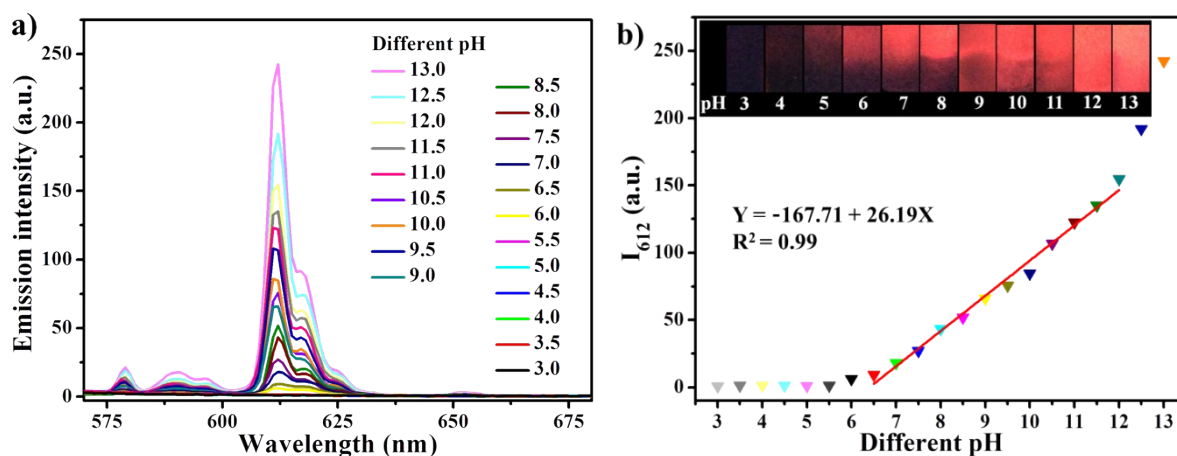


**Fig. S18.** **a)** The emission spectra of LMOF-1 loaded papers immersed in different pH aqueous solution ( $\lambda_{ex}=373$  nm, slits: 3/3 nm). **b)** The relationship between luminescent intensity at 612 nm and pH. Inset: Photos of the papers under UV light (365 nm) after soaked with different pH solution.

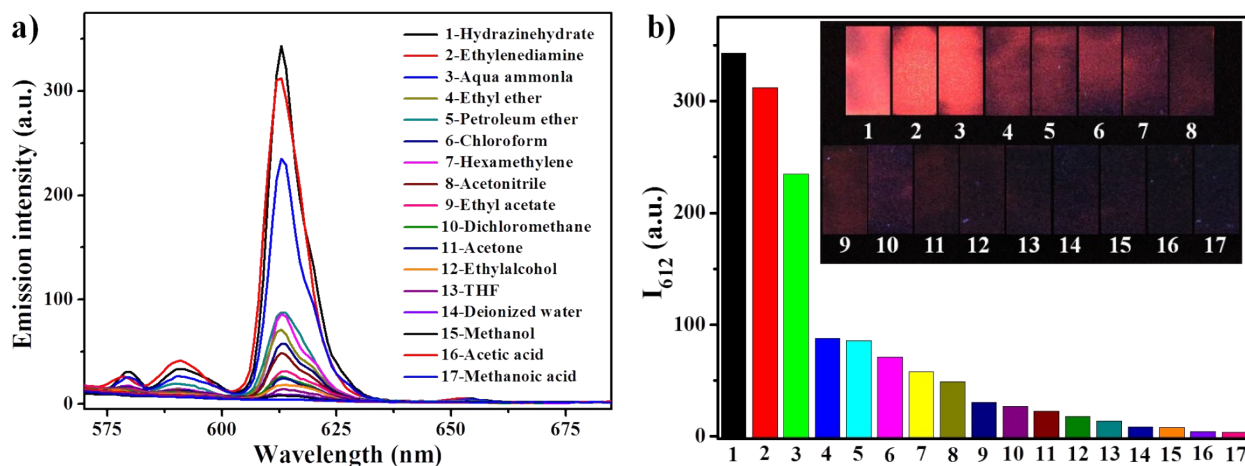


**Fig. S19.** **a)** The emission spectra of MOF-1 loaded papers processed in different vapors ( $\lambda_{ex}=373$  nm, slits: 3/5 nm). **b)** The emitting intensity at 612 nm (serial number corresponding to different vapors in **a)**). Inset: The digital photos of the tested papers under UV light (365 nm).

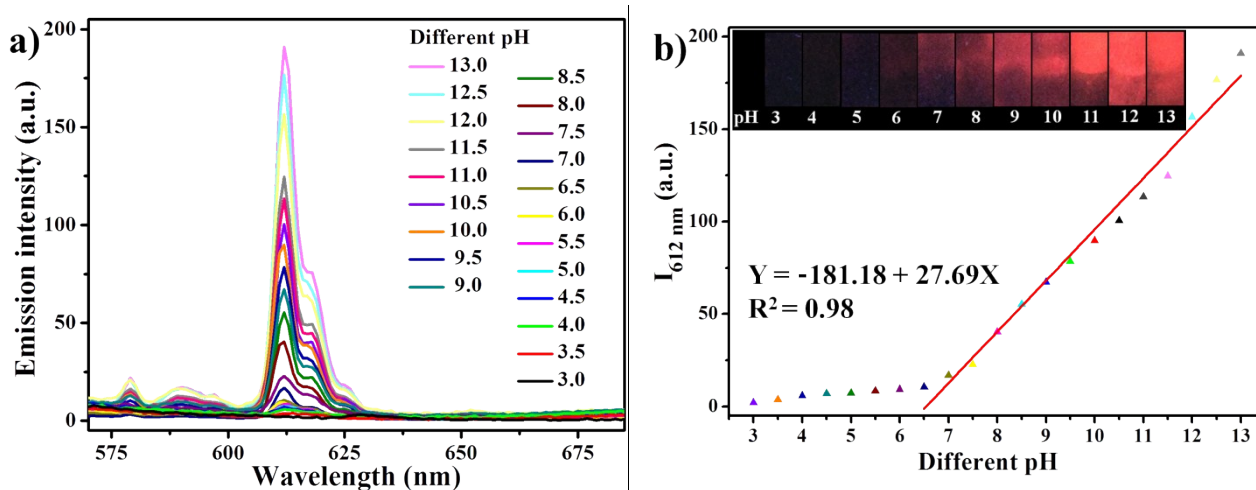


**Fig. S20.** **a)** The emission spectra of LMOF-1 loaded silica plates immersed in different pH aqueous solution ( $\lambda_{ex}=373$  nm, slits: 3/3 nm). **b)** The relationship between luminescent intensity at 612 nm and pH. Inset: Photos of silica plates under UV light (365 nm) after soaked with different pH solution.

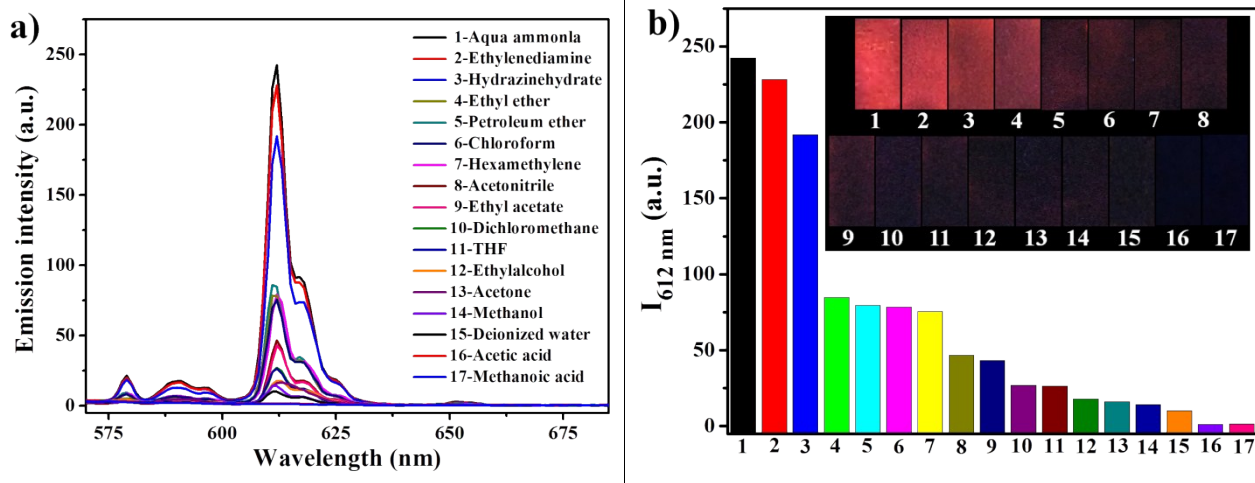


**Fig. S21. a)** The emission spectra of MOF-1 loaded silica plates processed in different vapors ( $\lambda_{ex}=373$  nm, slits: 3/3 nm). **b)** The emitting intensity at 612 nm (serial number corresponding to different vapors in a)). Inset: The digital photos of the tested silica plates under UV light (365 nm).

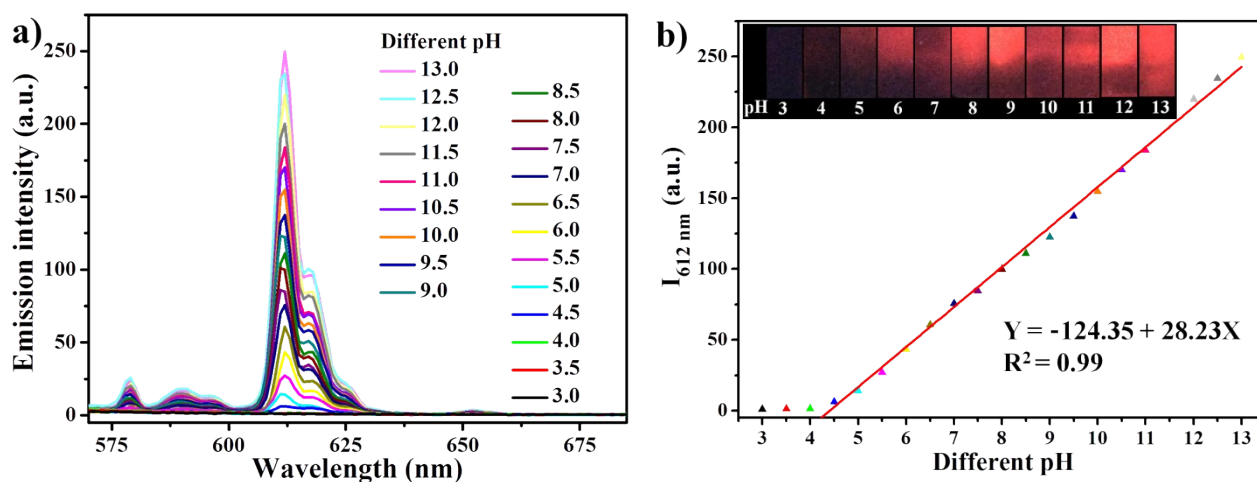


**Fig. S22. a)** The emission spectra of LMOF-2 loaded silica plates immersed in different pH aqueous solution ( $\lambda_{ex}=385$  nm, slits: 3/3 nm). **b)** The relationship between luminescent intensity at 612 nm and pH. Inset: Photos of silica plates under UV light (365 nm) after soaked with different pH solution.

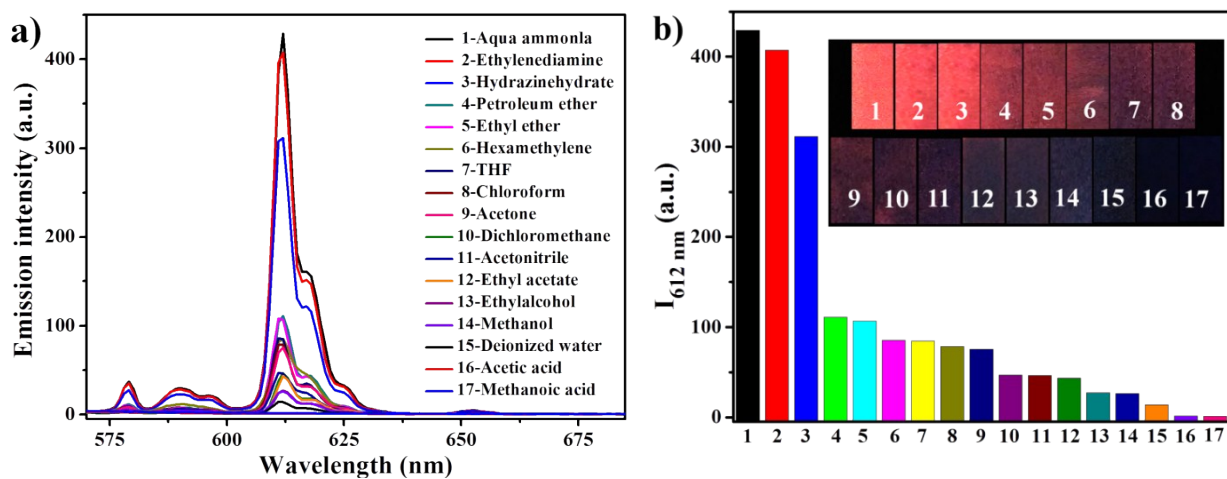


**Fig. S23.** **a)** The emission spectra of LMOF-2 loaded silica plates processed in different vapors ( $\lambda_{\text{ex}}=385$  nm, slits: 3/5 nm). **b)** The emitting intensity at 612 nm (serial number corresponding to different vapors in **a)**). Inset: The digital photos of the tested silica plates under UV light (365 nm).

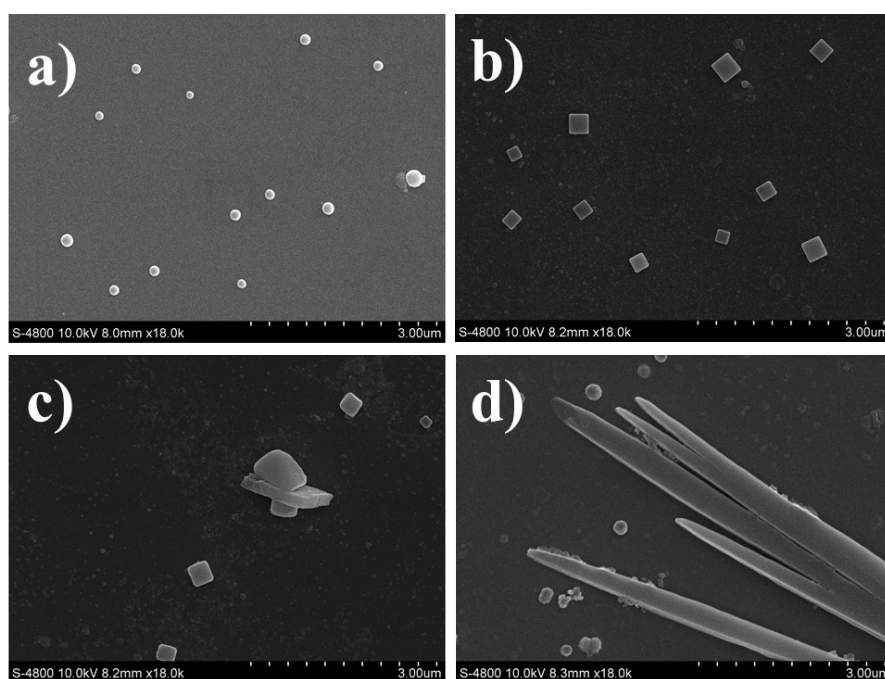


**Fig. S24.** The SEM of LMOF-1 in different pH solution. a) pH=3; b) pH=6; c) pH=9; d) pH=12.

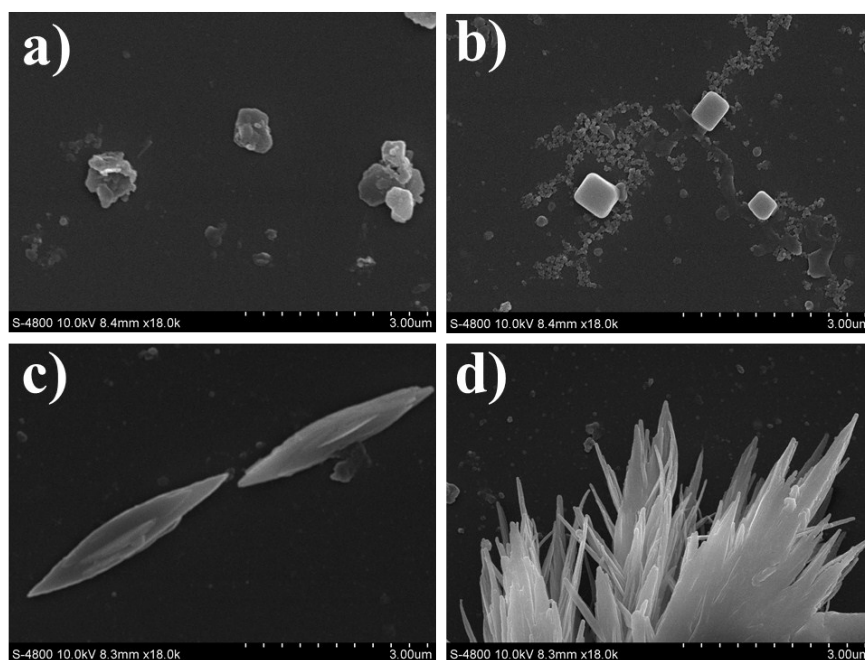


**Fig. S25.** The SEM of LMOF-2 in different pH solution. a) pH=3; b) pH=6; c) pH=9; d) pH=12.

As shown in **Fig. S24** and **S25**, different morphologies of LMOF-1 and LMOF-2 were observed in the condition of different pH values, which were due to the conformational transformation between enol and keto form in different acid-base environment<sup>1</sup> and Phen's and BPY's protonation and deprotonation under stronger acidic and alkalic circumstance.<sup>2-5</sup> In acidic environment, owing to the protonation of Phen and BPY as well as the ketonic transformation of DBM, LMOFs was damaged. So that crystal cannot generate (**Fig. S24a** and **S25a**). With the increase of pH value, crystal generated gradually, from block to strip (**Fig. S24b-d** and **S25b-d**).

## Reference

1. V. Pramod Kumar, K. Federico, S. Andreas, N. Patrick and B. Tobias, *J. Am. Chem. Soc.*, 2014, **136**, 14981-14989.
2. H. Doe, K. Yoshioka and T. Kitagawa, *J. Electroanal. Chem.*, 1992, **324**, 69-78.
3. Z. Yoshida and H. Freiser, *J. Electroanal. Chem.*, 1984, **162**, 307-319.
4. K. Dimitrou, A. D. Brown, K. Folting and G. Christou, *Inorg. Chem.*, 1999, **38**, 1834-1841.
5. A. Samotus, A. Kanas, W. Glug, J. Szklarzewicz and J. Burgess, *Transit. Metal Chem.*, 1991, **16**, 614-617.